

Electronic Supplementary Information

Synergetic optimization of electronic and thermal transport for high-performance thermoelectric GeSe-AgSbTe₂ alloy

Mingtao Yan^{a,b,‡}, Xiaojian Tan^{c,‡}, Zhiwei Huang^a, Guoqiang Liu^c, Peng Jiang^{a,*}, Xinhe Bao^{a,*}

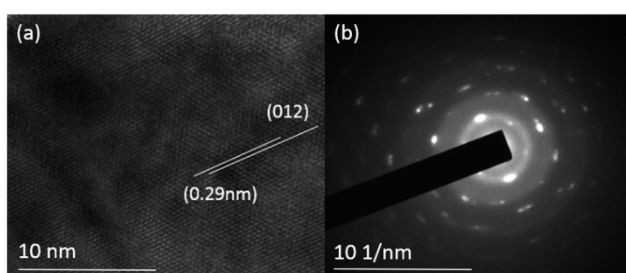


Fig. S1 (a) HRTEM image and (b) SAED pattern of GeSeAg_{0.2}Sb_{0.2}Te_{0.4}.

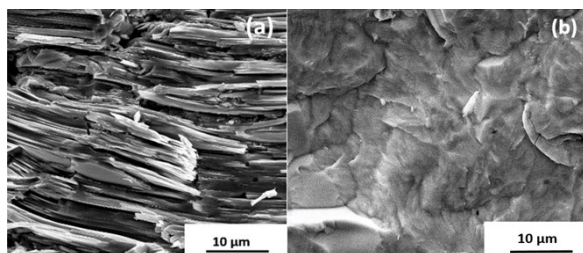


Fig. S2 SEM images of pure GeSe (a) and GeSe-20%AgSbTe₂ (b).

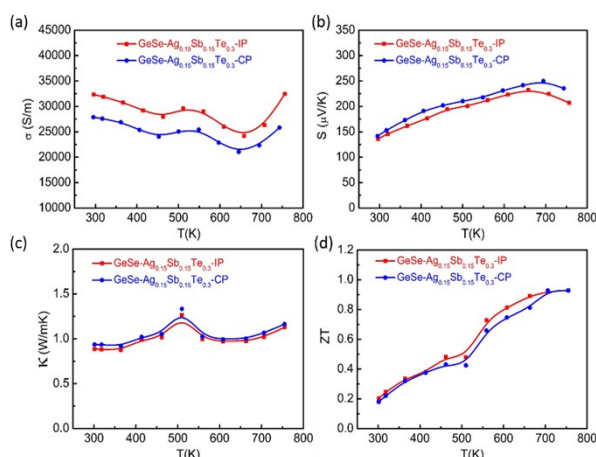


Fig. S3 Thermoelectric properties of GeSe-15%AgSbTe₂ along the directions perpendicular (IP) and parallel (CP) to the pressing direction.

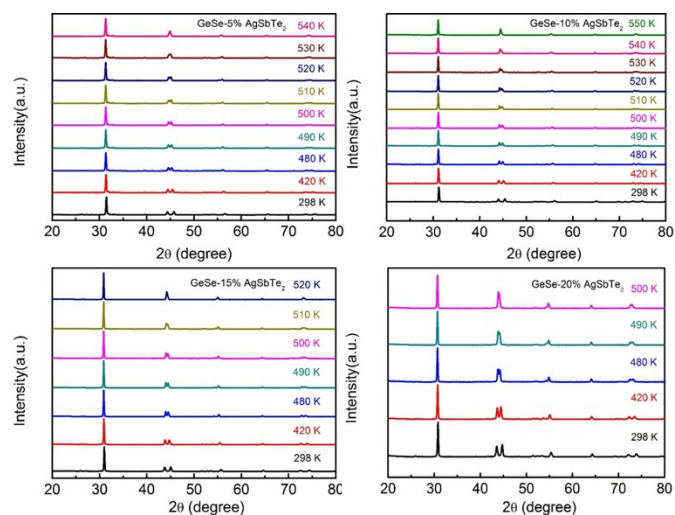


Fig. S4 Temperature-dependent powder XRD of GeSe-xAgSbTe₂ (x=5%, 10%, 15%, 20%).

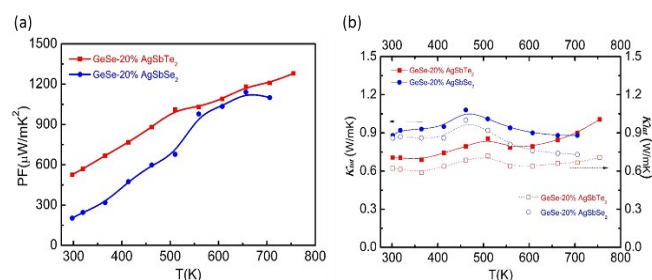


Fig. S5 Comparison of power factor (a) and thermal conductivity (κ_{tot} , κ_{lat}) (b) of GeSeAg_{0.2}Sb_{0.2}Te_{0.4} and GeSeAg_{0.2}Sb_{0.2}Se_{0.4}.

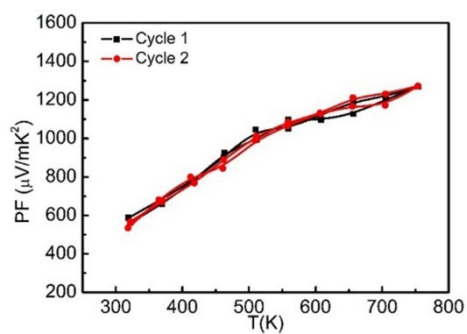


Fig. S6 Power factor of $\text{GeSeAg}_{0.2}\text{Sb}_{0.2}\text{Te}_{0.4}$ during two-cycle heating-cooling processes.

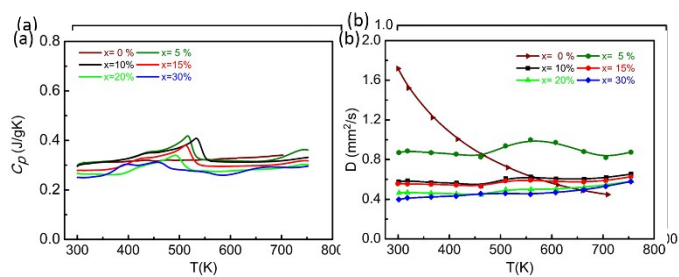


Fig. S7 Temperature dependence of heat capacity (a) and^f thermal diffusion coefficients (b) of GeSe-xAgSbTe_2 .